Fuel 356 (2024) 129610

Contents lists available at ScienceDirect

Fuel

journal homepage: www.elsevier.com/locate/fuel

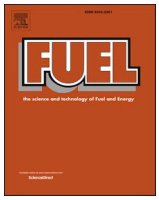

Full Length Article

Influence of carbon-coated zero-valent iron-based nanoparticle concentration on continuous photosynthetic biogas upgrading

Edwin G. Hoyos [a,b], Gloria Amo-Duodu [c], U. Gulsum Kiral [d], Laura Vargas-Estrada [e], Raquel Lebrero [a,b], Raúl Muñoz [a,b,*]

[a] Institute of Sustainable Processes, University of Valladolid, Dr. Mergelina, s/n, 47011 Valladolid, Spain
[b] Department of Chemical and Environmental Engineering, University of Valladolid, Dr. Mergelina, s/n, 47011 Valladolid, Spain
[c] Green Engineering and Sustainability Research Group, Department of Chemical Engineering, Faculty of Engineering and The Built Environment, Durban University of Technology, Durban 4001, South Africa
[d] Department of Environmental Engineering, Gebze Technical University, 41420 Kocaeli, Turkey
[e] Instituto de Energías Renovables, Universidad Nacional Autónoma de México, Temixco, Morelos CP. 62580, Mexico

ARTICLE INFO

Keywords:
Algal-bacterial photobioreactor
Biogas upgrading
CO_2 mass transfer
Microalgae productivity
Nanoparticles
Photosynthesis enhancement

ABSTRACT

This study assessed the influence of carbon-coated zero-valent nanoparticle concentration (70, 140 and 280 mg L^{-1}) on the performance of photosynthetic biogas upgrading in an indoor pilot scale plant composed of an algal-bacterial photobioreactor interconnected to an external biogas absorption column. In addition, the influence of nanoparticle concentration on the abiotic CO_2 gas-liquid mass transfer in the biogas absorption column was also evaluated. Microalgae productivity was enhanced by > 100 % when nanoparticles were added to the cultivation broth, which also boosted nitrogen and phosphorus assimilation from centrate. The biomethane produced complied with most international standards only when nanoparticles were supplemented, achieving CO_2 concentrations < 1 % (CO_2 removal efficiencies > 98 %) and CH_4 concentrations > 94 % in the treated biogas. Finally, this research consistently demonstrated that the improvement of biogas upgrading performance by the addition of nanoparticles was based on a photosynthesis enhancement or stimulation (which significantly increased the pH in the algal cultivation broth) rather than on an improved nanoparticle-mediated CO_2 capture in the biogas absorption column.

1. Introduction

Microalgae are microscopic photosynthetic organisms that can utilize sunlight and water to efficiently convert CO_2 into biomass with a concomitant uptake of dissolved nutrients and release of O_2. These microorganisms can grow in multiple environments such as wastewater, seawater, rivers and lakes. The optimum pH and temperature of most microalgae range from 7 to 9 and from 20 to 30 °C, respectively [1]. One of the main characteristics of microalgae is their wide variety of applications, which is often envisaged as one of the pillars of bioeconomy. Microalgae can be used as a biocatalyst for wastewater treatment, bioremediation, industrial gas cleaning and biogas purification, or as a feedstock for the production of food, animal feed, cosmetics, pharmaceuticals, biomaterials, biofertilizers/biostimulants or biofuels [2,3].

Microalgae production systems can be divided into open and closed photobioreactors. Open cultivation systems are typically implemented in artificial ponds, tanks, raceways and thin-layer platforms. On the other hand, closed systems are engineered as tubular loops, flat-panels and bubble columns [4]. Open raceway ponds or high-rate algal ponds (HRAPs) are a well-established photobioreactor configuration in industry for microalgae mass production that consume significantly less energy for mixing than tubular or flat panel photobioreactors [5,6]. However, due to the low biomass concentrations prevailing in these systems (typically ranging from 0.5 to 1.0 g L^{-1} to favour the penetration of light), microalgae harvesting is technically difficult and costly. Overall, the merits of HRAPs are versatility, low cost and ease of construction and operation, low maintenance costs and high durability [7]. However, HRAPs exhibit large areal requirements, high evaporation rates, poor accessibility of algae to light and susceptibility to microbial contamination [8].

During the last decades, HRAPs have been proposed as a technically feasible and sustainable alternative for the treatment of wastewaters [9].

* Corresponding author at: Institute of Sustainable Processes, University of Valladolid, Dr. Mergelina, s/n, 47011 Valladolid, Spain.
E-mail address: mutora@iq.uva.es (R. Muñoz).

https://doi.org/10.1016/j.fuel.2023.129610
Received 21 March 2023; Received in revised form 20 August 2023; Accepted 21 August 2023
Available online 26 August 2023

In recent years, pilot-scale studies have been carried out integrating photosynthetic biogas upgrading and wastewater treatment in HRAPs interconnected to an external CO_2-H_2S absorption column under both natural (outdoor) and artificial (indoor) illumination [10–15]. In these systems, algal-bacterial consortia (composed of sulphur-oxidizing, nitrifying and heterotrophic bacteria in symbiosis with microalgae and cyanobacteria) are used to fix the CO_2 from biogas, assimilate nitrogen and phosphorus from digestate, and oxidize H_2S and NH_4^+. This green process, operating at high alkalinities, can deliver a biomethane complying with most international regulations ($CH_4 \geq 90$ %, $CO_2 \leq 2$–4 %, $O_2 \leq 1$ %, and negligible amounts of H_2S) to be injected into natural gas networks or used as vehicle fuel [16,17].

One of the critical limitations in the industrial application of microalgae is the high cost of microalgae cultivation due to the limited photosynthetic efficiency and costly CO_2 mass transfer [18], since pH > 9 and alkalinity > 1000 mg IC L^{-1} are required to obtain a good efficiency of CO_2 gas–liquid mass transfer (> 90 %), which entails a significant consumption of chemicals [17,19]. In recent years, multiple techniques and strategies have been investigated with the aim of achieving higher microalgal productivities [20]. In this context, the addition of nanoparticles during microalgae cultivation has emerged as a promising method to enhance both CO_2 absorption efficiency and the efficient light conversion in the photobioreactor, thus improving microalgae growth [21]. Vargas-Estrada et al. [22,23] investigated the influence of different types of nanoparticles on batch microalgae cultures devoted to photosynthetic biogas upgrading. These studies demonstrated that the addition of the nanoparticles tested (Fe_2O_3, SiO_2 and carbon-coated zero-valent iron) improved both CO_2 absorption and microalgae growth. Similarly, Vargas-Estrada et al. [24] recently conducted a preliminary study to evaluate the influence of the addition of carbon-coated zero-valent iron nanoparticles at 70 mg L^{-1} to algal-bacterial cultures on the performance of photosynthetic biogas upgrading under continuous operation. The results showed that the addition of nanoparticles significantly boosted microalgae growth and increased the pH of the cultivation broth, thus enhancing the performance of photosynthetic biogas upgrading. Despite these promising results, the understanding of the mechanisms and key operational parameters in nanoparticle-aided photosynthetic biogas upgrading is limited. In this regard, three hypothetical mechanisms related to the improvement of CO_2 gas–liquid mass transfer (and consequently enhancement of biogas upgrading) have been proposed: shuttle effect, hydrodynamic effect and bubble breaking effect [23]. Furthermore, nanoparticles can boost the CO_2 availability in the cultivation broth and its assimilation by microalgae cultures, thus improving photosynthesis [22,23].

This study aimed at evaluating the effect of carbon-coated zero-valent iron-based nanoparticle concentration on the performance of an indoor pilot scale HRAP devoted to the continuous photosynthetic upgrading of biogas. In addition, the influence of nanoparticle concentration on the abiotic CO_2 gas–liquid mass transfer in the biogas absorption column was investigated.

2. Materials and methods

2.1. Experimental set-up

The photosynthetic biogas upgrading experimental set-up (indoor pilot plant) was composed of a 1.2 m^2 180 L HRAP (length = 170 cm; width = 82 cm; depth = 15 cm) interconnected to an external 2.5 L absorption column via an external liquid recirculation of the supernatant from an 8 L settler (Fig. 1a). The HRAP, with two water channels divided by a central wall and baffles in each side of the curvature, was constantly illuminated with LED lights (Phillips, Spain) and continuously mixed by a six-blade paddle wheel at an internal liquid recirculation velocity of approximately 0.2 m s^{-1}. The absorption column (AC) was a transparent PVC bubble column (internal diameter = 4.4 cm; height = 165 cm) provided with a metal gas diffuser (2 μm pore size) at the bottom.

A second experimental set-up consisting mainly of an absorption column with the same characteristics as the one described above, and a peristaltic pump (Watson Marlow, UK), was used to evaluate the influence of nanoparticle concentration on the CO_2 gas–liquid mass transfer in the biogas absorption column under abiotic conditions (Fig. 1b).

2.2. Biogas, centrate and nanoparticles

A synthetic gas mixture containing CH_4 (70 %), CO_2 (29.5 %) and H_2S (0.5 %) (Abello Linde, Spain) was used as a model biogas. Real centrate was used as a source of nutrients and water. This centrate was obtained from the centrifugation of the effluent from the mixed sludge digesters of the Wastewater Treatment Plant (WWTP) of Valladolid (Spain) and was stored at 4 °C before use. Carbon-coated zero valent iron nanoparticles (NPs) obtained from CALPECH (Spain) were sonicated to prevent nanoparticle agglomeration and facilitate their addition to the microalgae cultivation [22]. A Sonorex Digitec (Bandelin, Germany) operated at 30 kHz for 1 h was used for ultrasonication in order to disperse the NPs in the centrate. CALPECH NPs (containing 8.68 % wt of Fe) exhibited a BET surface area of 27.3 m^2 g^{-1}, a pore volume of 0.28 cm^3 g^{-1} and an average pore diameter of 41.5 nm (mesoporous material according to the IUPAC classification) [24]. The centrate containing the target concentrations of NPs was continuously stirred using a magnetic agitator during feeding to the HRAP. The influence of nanoparticle concentration on the CO_2 gas–liquid mass transfer was investigated using a synthetic centrate whose chemical composition was: 3.5 g L^{-1} of $NaHCO_3$, 1.5 g L^{-1} of NH_4Cl, 0.39 g L^{-1} of CH_4N_2O, 0.731 g L^{-1} of K_2HPO_4, 0.0175 g L^{-1} of NaCl, 0.01 g L^{-1} of $CaCl_2$ and 0.056 g L^{-1} of $MgSO_4$.

2.3. Influence of nanoparticle concentration on photosynthetic biogas upgrading

This study was carried out from March the 7th to September the 16th 2022 (~200 days) and was divided into three different stages. During stage I (days 0 to 36), the NPs concentration in the cultivation broth and centrate was set at 70 mg L^{-1}, and biomass harvesting rate was maintained at 33.0 g m^{-2} d^{-1} according to [24]. During stage II (days 37–95) and stage III (days 96–194), the NPs concentration in the cultivation broth and centrate was set at 140 and 280 mg L^{-1}, respectively, with biomass harvesting rates of 48.2 g m^{-2} d^{-1} in both stages. At this point, it should be noted that the effect of NPs concentrations ranging between 70 and 280 mg L^{-1} have not been tested in batch experiments [22,23] and needs further study. The HRAP was initially inoculated with an algal-bacterial consortium (obtained from a previous experiment [24]) with *Chlorella* sp. as the dominant microalgal species. The bacteria present in the consortium were nitrifying, sulphur-oxidizing and consuming organic matter, but their molecular identification was out of the scope of this study. During the entire experimental period, the system was continuously fed with 4.3 L d^{-1} of centrate supplemented with 7.3 g d^{-1} of sodium carbonate to counteract the active inorganic carbon consumption in the HRAP mediated by the enhanced microalgae growth following nanoparticle addition. Biomass recirculation from the bottom of the settler to the HRAP was set at 7.2 L d^{-1} according to Posadas et al. [15] to improve the settleability and avoid the degradation of the algal-bacterial biomass in the settler. The flow rate of synthetic biogas supplied to the AC was 60 L d^{-1}. The biogas load was estimated based on the biogas composition (29.5 % CO_2), the HRAP surface area (1.2 m^2), the illumination intensity and regime, to support a microalgae productivity of 22.5 g m^{-2} d^{-1}. Similarly, the centrate load was determined by the algal productivity set and the composition of the centrate in terms of inorganic carbon and nitrogen concentration (more details can be found in Supplementary Material). The recycling liquid/gas (L/G) ratio in the AC was fixed at 2 according to literature studies in a similar

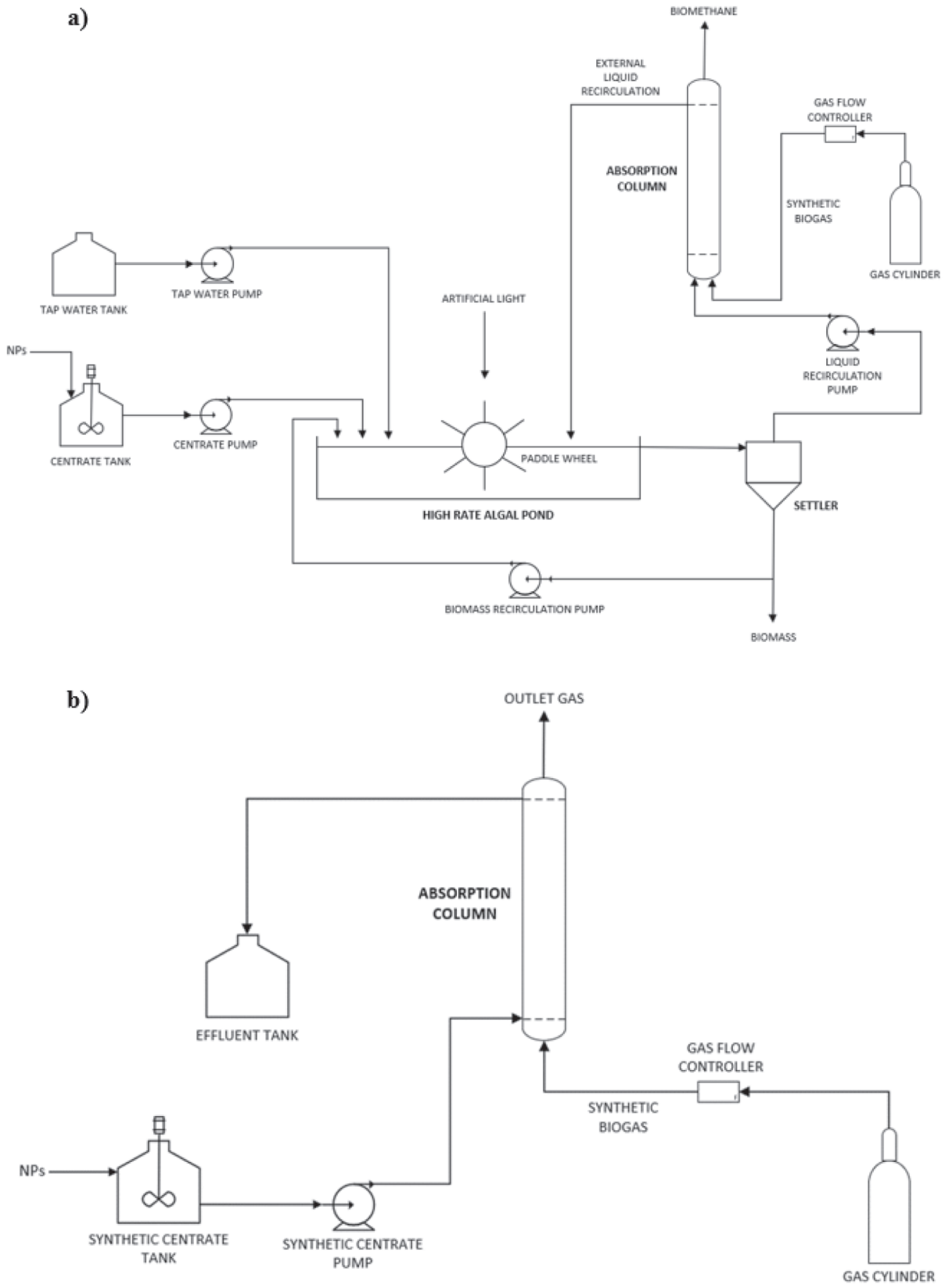

Fig. 1. Schematic diagrams of a) the photosynthetic biogas upgrading experimental set-up and b) the abiotic biogas absorption column set-up.

experimental set-up [13,14,25]. L/G ratio of 0.5–1 are typically set when the HRAP is operated at pH > 9 and inorganic carbon concentrations > 1200 mg IC L^{-1}, conditions that guarantee an effective CO_2 capture in the absorption column while minimizing O_2 and N_2 desorption. Tap water was supplied to the HRAP to compensate evaporation losses. The algal-bacterial biomass harvesting rate (W) (g m^{-2} d^{-1}) was controlled according to Eq. (1) [26]:

$$W = (TSS_{settler} \times Q_{wout})/S \quad (1)$$

where $TSS_{settler}$ is the biomass concentration at the bottom of the settler (g L^{-1}), Q_{wout} is the flowrate of the biomass harvested (L d^{-1}) and S is the HRAP surface (m^2). The algal-bacterial biomass was centrifuged for 10 min at 7800 rpm. It should be noted that during the entire experiment, the supernatant resulting from the centrifugation of the settled algal-bacterial biomass withdrawn to maintain a fixed biomass productivity, was returned to the HRAP (zero-effluent process). The photosynthetic active radiation (PAR) in the surface of the HRAP was maintained constant at 1406 ± 45 μmol m^{-2} s^{-1}. Ambient and HRAP temperatures averaged 26.3 ± 1.6 and 31.1 ± 1.2 °C, respectively (Fig. S1a).

Ambient and HRAP temperatures, dissolved oxygen concentration (DO) and pH in the HRAP, AC and centrate were daily monitored. PAR and the composition of the inlet and outlet gas streams in the AC were measured twice a week. Likewise, the concentrations of total suspended solids (TSS) and volatile suspended solids (VSS) in the HRAP and settler, and the concentrations of total organic carbon (TOC), inorganic carbon (IC), total nitrogen (TN), N-NH_4^+, N-NO_2^-, N-NO_3^-, P-PO_4^{3-} and S-SO_4^{2-} in the soluble fraction of the centrate and HRAP cultivation broth were monitored twice a week. Once per month, the algal-bacterial biomass was stored (after drying for 24 h at 105 °C) for elemental analysis, and for the morphological characterization of the algal population structure (one sample fixed with Lugol's solution at 5 % and another with neutral formaldehyde solution at 10 %, both stored at 4 °C).

The influence of NPs on the CO_2 gas–liquid mass transfer in the AC under abiotic conditions was carried out at 26 °C using the synthetic biogas described above. The flow rate of synthetic biogas and L/G ratio were set at 55 L d^{-1} and 2, respectively. A synthetic centrate with the composition above described and pH = 8 was used. Three different concentrations of NPs in the centrate (70, 150 and 300 mg L^{-1}) and a control (no NPs) were tested. Both the gas composition and the pH of the liquid at the outlet of the AC were measured under steady state, which was assumed after 3 times the hydraulic retention time of the liquid in the AC (~100 min). Gas and liquid samples were collected at 100, 115, 130, 145 and 160 min from the start of each experiment to ensure stable system conditions.

2.4. Analytical procedures

Temperature and DO in the culture broth of the HRAP were measured using an Oxi 3310 oximeter (WTW, Germany). pH was determined by using a SensION^{TM} + PH3 pHmeter (HACH, Spain). PAR in the HRAP was measured with a LI-250A light meter (LI-COR Biosciences, Germany). Liquid samples were centrifuged for 10 min at 7800 rpm (SIGMA 2-16P, Germany) and filtered through 0.7 μm glass fibre filters prior to TOC, IC and TN analysis using a TOC-V_{CSH} analyser equipped with a TNM-1 module (Shimadzu, Japan). In addition, liquid samples were filtered through 0.22 μm nylon filters for the analysis of nitrate, nitrite, phosphate and sulphate, which was carried out via HPLC-IC as described elsewhere [27]. N-NH_4^+ concentration was determined via the Nessler analytical method using a UV-2550 spectrophotometer (Shimadzu, Japan) at 425 nm. The gas concentrations of CH_4, N_2, O_2, CO_2 and H_2S were determined by GC-TCD according to Alcántara et al. [10]. The analysis of TSS and VSS concentrations was conducted according to Standard Methods [28]. The determination of elemental composition of the algal-bacterial biomass (C, N and P) and microalgae population structure was performed as described elsewhere [29]. The removal efficiency of CO_2 was calculated according to [26]. Nitrogen and phosphorus recovery from centrate by assimilation into biomass (RE_x) was calculated according to Eq. (2):

$$RE_x(\%) = (W \times X)/(Q_{in} \times C_{in}) \quad (2)$$

where Q_{in} represents the centrate flowrate (L d^{-1}), C_{in} the concentrations in the centrate of N and P (mg L^{-1}), W the biomass harvesting rate expressed in mg d^{-1} and X corresponds to the content of nitrogen and phosphorus in the harvested biomass (%).

2.5. Statistical data treatment

The results are shown as mean values ± standard deviation. A one-way ANOVA analysis (at 95 % confidence level) was performed to assess the statistical significance of the mean difference.

3. Results and discussion

3.1. Influence of nanoparticle concentration on HRAP performance

The water evaporation rate in the HRAP during the entire experiment averaged 11.1 ± 0.6 L m^{-2} d^{-1} (Fig. S1b). This high evaporation rate compared to those estimated by Guieysse et al. [30] in temperate climates in open ponds under outdoors conditions (1.3–6.2 L m^{-2} d^{-1}) was likely promoted by the high temperatures and high turbulence prevailing in the pilot HRAP cultivation broth [25,31].

3.1.1. pH, DO, VSS and microalgae population

The control scenario (absence of nanoparticles) was previously published [24]. During stages I and II, the predominant microalgae population in the cultivation broth was *Chlorella* sp. When the HRAP was operated at a NPs concentration of 70 mg L^{-1}, the average value of pH, DO and VSS in the HRAP under steady state was 9.00 ± 0.05 (days 8–36), 11.53 ± 1.07 mg O_2 L^{-1} and 1.38 ± 0.21 g L^{-1} (days 1–36 for both), respectively (Fig. 2). An increase in NPs concentration in the HRAP cultivation broth and centrate from 70 to 140 mg L^{-1} caused a rapid and significant increase in pH and VSS up to steady state values of 9.22 ± 0.03 (days 82–95) ($p = 1.3 \times 10^{-8}$ and $n = 10$) and 3.10 ± 0.15 g L^{-1} (days 78–95) ($p = 4.4 \times 10^{-14}$ and $n = 10$), respectively, which was probably mediated by an increase in photosynthetic activity and therefore in algal growth (Fig. 2 a & c). DO initially increased substantially but it stabilized at a slightly lower value (11.02 ± 1.21 mg O_2 L^{-1}) (days 50–95) compared to the steady state value in stage I (Fig. 2b). This phenomenon induced an outstanding increase in biomass productivity of almost 50 % (from 33.0 to 48.2 g m^{-2} d^{-1}) when NPs concentration increased from 70 to 140 mg L^{-1}, and enhancements higher than 100 % compared with process operation in the absence of NPs (from 22.5 to 48.2 g m^{-2} d^{-1}) [24]. The new biomass harvesting rate (48.2 g m^{-2} d^{-1}) was set from day 54 onwards, and calculated based on the increase in VSS during the first 5 sampling points in stage II. Indeed, the number of *Chlorella* sp. cells/mL increased from 1.77×10^6 in stage I to 2.51×10^6 in stage II, further supporting the fact that the increase in NPs concentration from 70 to 140 mg L^{-1} induced a significant increase in the microalgae production performance of the process. It is important to note that most of the biomass present in the cultivation broth corresponds to photosynthetic microorganisms since the centrate does contain mainly recalcitrant organic carbon and ammonium, and the yield of both nitrifying and sulfur oxidizing bacteria is low.

Interestingly, microalgae growth decreased in stage III (when the NPs concentration in the system was increased from 140 to 280 mg L^{-1}), as suggested by the progressive decline in pH, DO and VSS concentrations of the cultivation broth from day 104 till day 137 (Fig. 2). However, microalgae activity gradually recovered by the end of stage III and the pH, DO and VSS concentrations finally stabilized at 9.53 ± 0.10, 10.79 ± 1.25 mg O_2 L^{-1} (days 152–194 for both) and 2.92 ± 0.17 g L^{-1} (days 165–194), respectively. This fact can be attributed to the change of

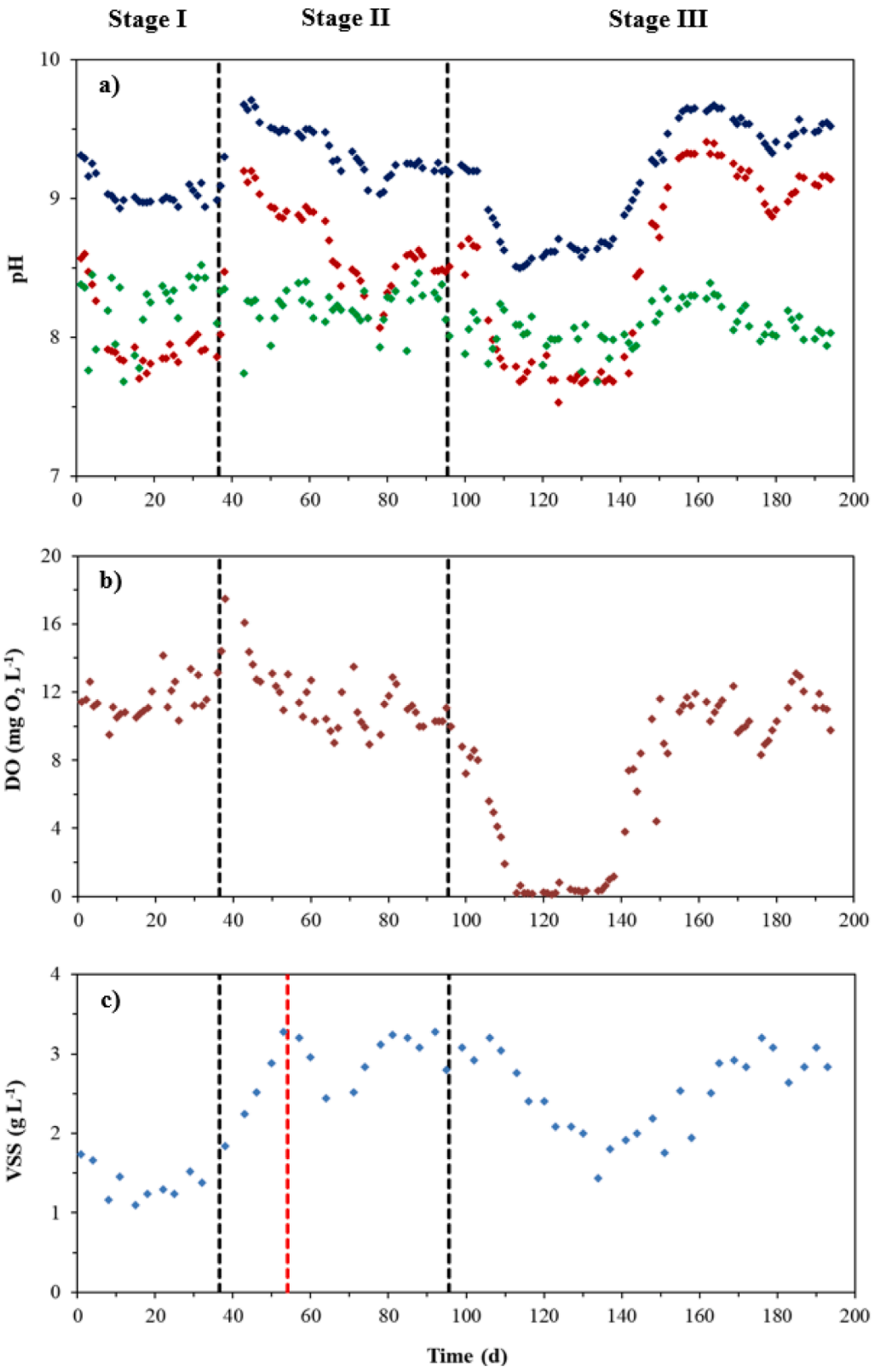

Fig. 2. Time course of a) pH of HRAP (blue diamonds), AC (red diamonds), and centrate (green diamonds); b) dissolved oxygen concentration in the HRAP; and c) microalgal biomass concentration in the HRAP. NPs concentration: Stage I → 70 mg L^{-1}, Stage II → 140 mg L^{-1} and Stage III → 280 mg L^{-1}. From red dashed line (chart c - day 54), the biomass harvesting rate was changed from 33.0 to 48.2 g m^{-2} d^{-1}.

the dominant microalgal species from *Chlorella* sp. to *Chloroidium saccharophilum* likely induced by ionic strength (or alkalinity) accumulation in the system as a consequence of the zero effluent operating mode. A similar algae population replacement was also observed by Posadas et al. [15] in a comparable experimental set-up under outdoor conditions, likely as a result of the recirculation of the settled biomass (to improve species control and harvesting efficiency) and the high alkalinity in the cultivation broth. The addition of nanoparticles substantially increased the pH in the cultivation broth (from 8.55 to 9.53) as well as the biomass production, which resulted in a considerable increase in the VSS concentration in the HRAP (from 1.56 to 3.10 g L^{-1}) and productivity (from 22.5 to 48.2 g m^{-2} d^{-1}) compared to previously published control scenario in the absence of NPs [24]. The mean DO values under steady state in the three operational stages were similar and remained below inhibitory levels (typically above 25 mg O_2 L^{-1}) (Fig. 2b) [15]. The pH values in the biogas absorption column were lower than those recorded in the HRAP (Fig. 2a) as a result of the acidification of the recirculating liquid mediated by the active absorption of CO_2 and H_2S from biogas [15,26]. The pH of the centrate supplemented with 7.3 g d^{-1} of Na_2CO_3 remained constant at 8.22 ± 0.19 throughout stages I and II (Fig. 2a). Interestingly, the pH of the centrate decreased to 8.07 ± 0.15 during stage III due to an intensification of the partial nitrification process (biologically oxidizing ammonia into nitrite) in this stage as a result of the growth of a biofilm in the feeding tank

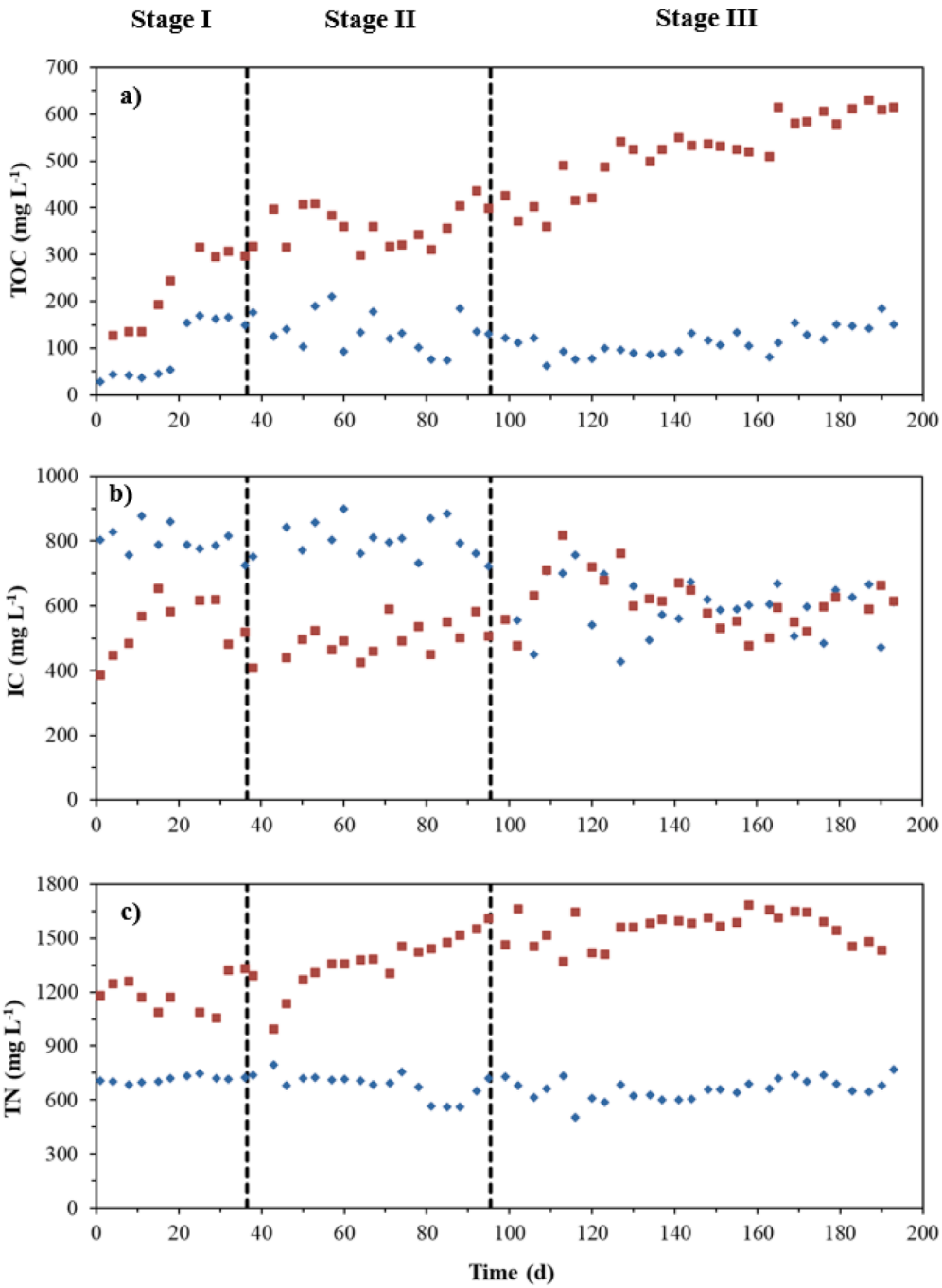

Fig. 3. Time course of a) TOC, b) IC and c) TN concentrations in the HRAP (red squares) and centrate (blue diamonds). NPs concentration: Stage I → 70 mg L^{-1}, Stage II → 140 mg L^{-1} and Stage III → 280 mg L^{-1}.

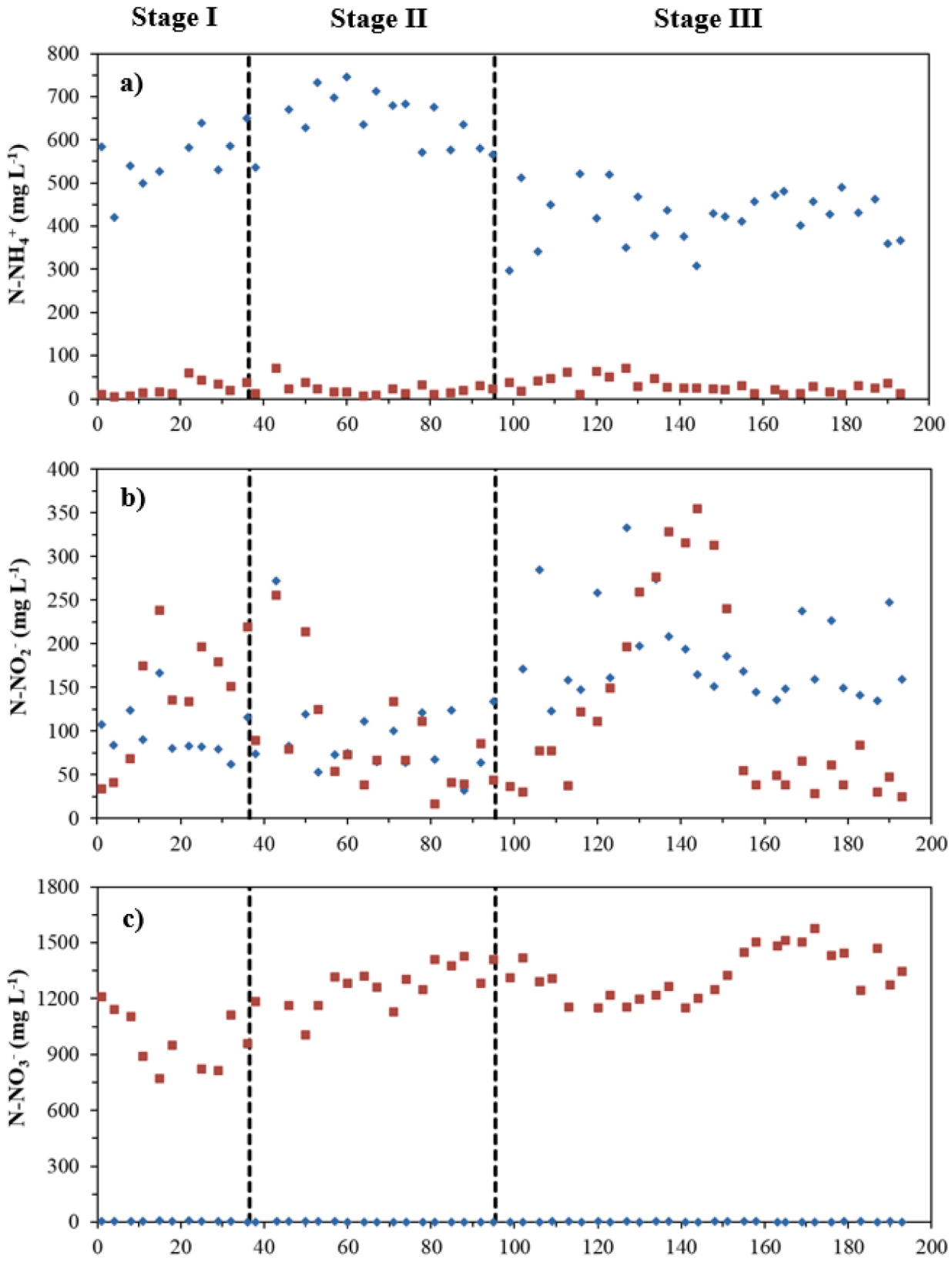

Fig. 4. Time course of a) $N\text{-}NH_4^+$, b) $N\text{-}NO_2^-$, c) $N\text{-}NO_3^-$, d) $P\text{-}PO_4^{3-}$ and e) $S\text{-}SO_4^{2-}$ concentrations in the HRAP (red squares) and centrate (blue diamonds). NPs concentration: Stage I → 70 mg L^{-1}, Stage II → 140 mg L^{-1} and Stage III → 280 mg L^{-1}.

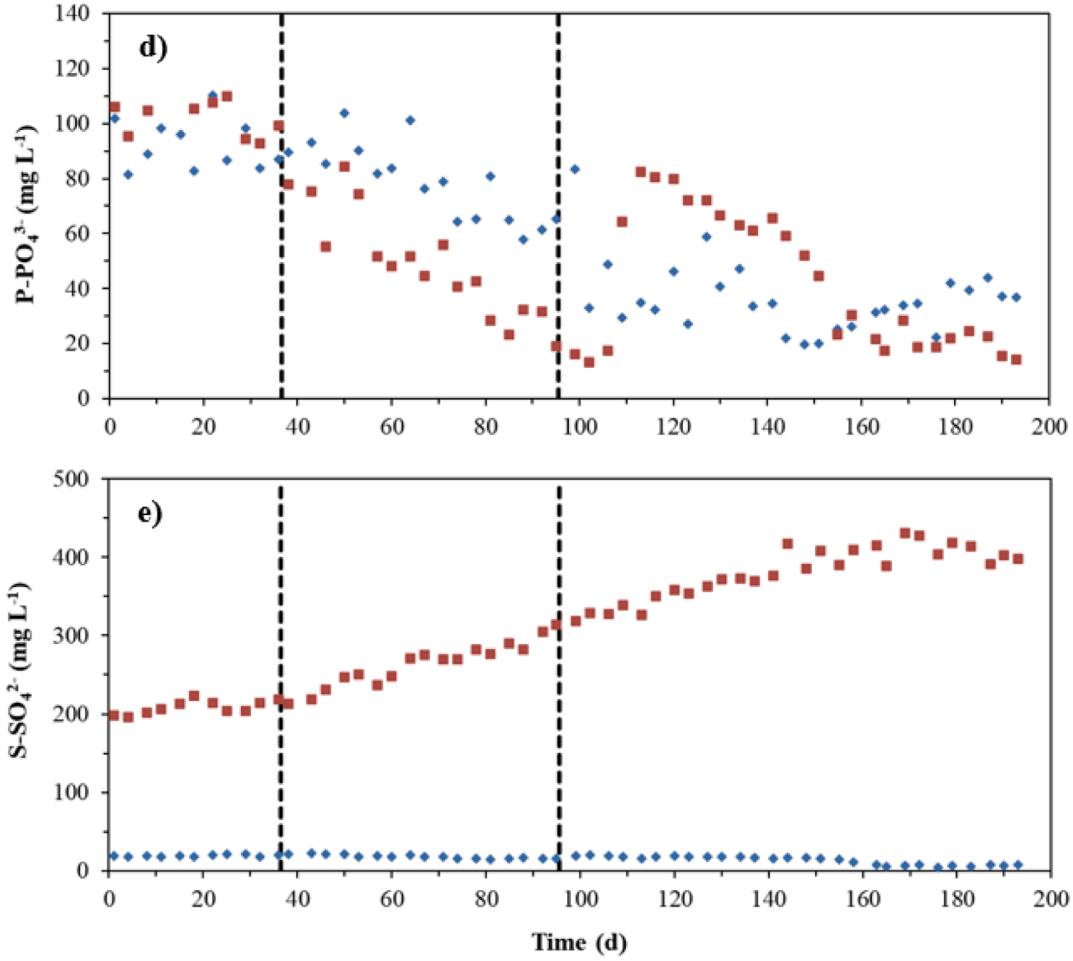

Fig. 4. (*continued*).

(Fig. 4b).

3.1.2. TOC, IC and alkalinity

The average TOC concentration in the centrate during the entire experiment was 117 ± 42 mg L^{-1} (Fig. 3a), which remained within the typical concentration values of TOC in domestic wastewater (80–260 mg L^{-1}) [32]. However, the dissolved organic carbon in digestates/centrates is typically composed of recalcitrant compounds, since most of the easily biodegradable carbon is removed during anaerobic digestion [33]. The gradual increase in TOC concentration in the culture broth of the HRAP from the beginning (127 mg L^{-1}) to the end (616 mg L^{-1}) of the experiment (Fig. 3a) was likely due to the accumulation of recalcitrant organic matter either released by the metabolism of microalgae during their photoautotrophic growth and by the lysis of the algal-bacterial biomass present in the culture broth [11,27] or accumulated from the centrate as a result of the zero-effluent operational mode set in this work.

On the other hand, the average IC concentration in the centrate (supplemented with 1.7 g L^{-1} of Na_2CO_3) during stages I, II and III was 801 ± 44, 805 ± 54 and 596 ± 85 mg L^{-1}, respectively (Fig. 3b). The substantial decrease in IC concentration in the centrate during stage III was associated to the decrease in the pH (induced by the partial NH_4^+ nitrification observed) of the centrate during this stage (Fig. 2a), which shifted the equilibrium towards CO_2 and thus promoted the subsequent desorption of IC into the atmosphere. The IC concentration in the HRAP during stage I increased slightly from 385 to 520 mg L^{-1}. During stage II, this parameter remained constant at average values of 495 ± 53 mg L^{-1}, which entailed that the mass flow rate of inorganic carbon entering the system through the centrate and the AC (as a result of the CO_2 gas–liquid mass transfer) and CO_2 absorbed from the atmosphere into the HRAP cultivation broth matched the mass flow rate of inorganic carbon consumed by the microalgae and nitrifying bacteria. During stage III, the IC concentration in the HRAP initially increased likely mediated by the deterioration in photosynthetic activity and then decreased as a consequence of the change in the microalgae population structure to finally stabilize at 569 ± 53 mg L^{-1} (days 148–194) (Fig. 3b). Dissolved inorganic carbon remained at low concentrations (~500 mg IC L^{-1}) probably due to the significant photosynthetic activity mediated by the addition of NPs.

Alkalinity accumulation could have occurred in the HRAP due to the daily addition of a substantial amount of sodium carbonate in the centrate and the zero effluent operating strategy. Theoretically, CO_2 dissolution and desorption do not change the alkalinity of the liquid and photosynthesis could rather increase alkalinity (especially when nitrate is the major nitrogen source in the medium) [34]. On the other hand, assimilation of ammonia, as well as nitrification, is known to reduce alkalinity [35]. Alkalinity accumulation could have a significant effect on photosynthetic activity and CO_2 absorption. However, the contribution of such accumulation to the increase in photosynthesis when NPs concentration was stepwise increased from 70 to 140 mg L^{-1} can be neglected due to the rapid and significant response of the system to such a change. On the other hand, plausibly, the reduction in biomass production observed in stage III may have stemmed from the accumulation of ionic strength (or alkalinity), recovering by the end of stage III via a

shift in algal community structure towards ionic strength-resilient species.

3.1.3. TN, ammonium, nitrite and nitrate

The concentrations of TN (Fig. 3c) and N-NO_3^- (Fig. 4c) in the centrate during the entire experiment averaged 680 ± 59 and 3 ± 2 mg N L^{-1}, respectively. Most of the dissolved nitrogen in the centrate was in the form of ammonium. The average concentration of N-NH_4^+ in the feed during stages I, II and III was 556 ± 68, 646 ± 44 and 424 ± 61 mg L^{-1}, respectively (Fig. 4a). The substantial decrease in the ammonium concentration in the feed during stage III compared to stages I and II was due to a marked increase in the bacterial partial nitrification. N-NO_2^- concentration in the centrate was similar during stages I and II (98 ± 29 and 96 ± 54 mg L^{-1}, respectively), and increased substantially during stage III (188 ± 54 mg L^{-1}) (Fig. 4b). The high ambient temperature conditions and the continuous agitation, along with the formation of a bacterial biofilm in the feeding tank promoted the bacterial partial oxidation of N-NH_4^+ to N-NO_2^- both in the feed and in the HRAP (Fig. 4b) [36,37].

The TN concentration in the cultivation broth of the HRAP increased from the beginning (1182 mg L^{-1}) to the end (1434 mg L^{-1}) of the experiment (Fig. 3c). This fact was likely due to the accumulation of organic nitrogen mediated by microalgal-bacterial metabolite excretion and cell lysis under the zero effluent strategy tested [10]. N-NH_4^+ concentration in the cultivation broth of the photobioreactor remained almost negligible throughout the experiment (Fig. 4a). Comparable results were obtained in analogous experimental set-ups using centrates with a high ammonium loading [14,15,26]. Nitrogen stripping as NH_3 could be also responsible for NH_4^+ removal (apart from nitrification and assimilation into biomass) due to the high pH prevailing in the cultivation broth [38]. Most of the TN in the HRAP cultivation broth was present in the form of nitrate (Fig. 4c). Therefore, despite the high temperatures in the cultivation medium (29–33 °C), the complete nitrification of NH_4^+ by the nitrifying bacterial community prevailed over the partial nitrification to nitrite likely due to the high DO (10.8–11.5 mg L^{-1}) supported by algal photosynthesis [25,29]. Nitrate accumulation from the beginning (1210 mg N L^{-1}) to the end (1345 mg N L^{-1}) of the experiment (Fig. 4c) was very low probably because of the high photosynthetic activity driven by nanoparticle supplementation, which increased nitrogen uptake from the cultivation broth.

3.1.4. Phosphate and sulphate

The concentration of P-PO_4^{3-} in the centrate during stages I, II and III averaged 92 ± 9, 79 ± 14 and 36 ± 13 mg P L^{-1}, respectively (Fig. 4d). These substantial deviations of the phosphate concentration in the centrate can be explained by variations in the operation of Valladolid WWTP. Phosphate concentration in the photobioreactor remained constant during stage I (102 ± 6 mg P L^{-1}). During stage II, phosphate concentration substantially decreased to 19 mg P L^{-1} due to the rapid increase in microalgae growth mediated by the higher NPs concentration in the system (140 mg L^{-1}). By day 107 (stage III), P-PO_4^{3-} concentration in the HRAP was increased via external addition of K_2HPO_4 to prevent phosphate limitation (< 3 mg P L^{-1}) [13]. From day 113 (stage III), P-PO_4^{3-} concentration substantially decreased as a result of the recovery of microalgal activity and high biomass production promoted by NPs addition and to a lesser extent due to the gradual reduction in the phosphate content of the centrate, and stabilized at 22 ± 5 mg P L^{-1} by the end of the stage III (days 155–194). On the other hand, the mean concentration of S-SO_4^{2-} in the centrate throughout the experiment was 16 ± 5 mg L^{-1} (Fig. 4e). The concentration of S-SO_4^{2-} in the HRAP increased from ~ 200 to ~ 400 mg L^{-1}, since the H_2S continuously transferred from biogas was oxidized to sulfate by sulphur-oxidizing bacteria [12], and accumulated in the system triggered by the zero-effluent operational mode.

Table 1
Elemental composition of the algal-bacterial biomass. NPs concentration: Stage I → 70 mg L^{-1}, Stage II → 140 mg L^{-1} and Stage III → 280 mg L^{-1}.

Stage	Biomass elemental composition (%)		
	C	N	P
I	32.1	5.7	1.7
II	39.3	6.9	1.9
III	38.1	6.1	1.4

Values are given at the end of the stage.

3.1.5. Algal-bacterial biomass composition, phosphorus and nitrogen recovery and possible fate of NPs

The C, N and P contents in the biomass (Table 1) were in agreement with those reported in the literature ([11,15]). The biomass C/N ratio remained constant at 5.8 ± 0.3 regardless of the operational stage and very close to the optimal ratio for microalgae growth of 5.6 according to [25]. Phosphorus recovery from centrate via biomass assimilation accounted for 187 ± 21 %, 188 ± 20 % and 200 ± 25 % during stages I, II and III, respectively, while nitrogen recovery accounted for 82 ± 6 %, 136 ± 15 % and 124 ± 13 % during stages I, II and III, respectively. The fact that phosphorus recovery remained above 100 % could be due to the fact that organic phosphorus was not measured in this experiment, and the calculations were done with phosphate, which might entail an underestimation of the real phosphorus removed. In a practical situation, the typical composition of centrates entails that nitrogen is the limiting nutrient and phosphate concentration tends to accumulate in the algal-bacterial broth. In this particular scenario, process operation at pH of 9.5–10 would support the conditions for phosphorus precipitation and its further removal with the wasted biomass.

Despite the relevance of this issue, the fate of NPs was out of the scope of this study. Based on their carbonaceous recalcitrant structure, it can be hypothesized that NPs would be attached to the microalgae cell wall and leave the system during biomass harvesting. Further investigation should be devoted to elucidate this particular issue, which determines the potential valorization routes of the algal-bacterial biomass generated during photosynthetic biogas upgrading.

3.2. Effect of NPs concentration on the biomethane produced

The steady state CO_2 concentrations in the biomethane produced averaged 3.1 ± 1.2 %, 1.7 ± 0.9 %, and 0.8 ± 0.3 % (days 145–194) in stages I, II and III, respectively (Fig. 5a). This corresponded to removal efficiencies of CO_2 (RE-CO_2) of 91.4 ± 3.2 %, 95.9 ± 2.1 % and 98.1 ± 0.7 % during stages I, II and III, respectively. The decrease in the CO_2 concentration in the biomethane produced from stage I to III was likely mediated by the increase in pH from 9.00 (stage I) to 9.22 (stage II) and to 9.53 (stage III). In this context, the CO_2 mass transfer in the absorption column is governed by operational parameters such as pH, alkalinity and L/G ratio, but also by design parameters such as the sparged bubble size and column dimensions (height and diameter). Thus, Marín et al. [39] achieved a minimum biomethane CO_2 concentration of 13.5 % v/v (RE-CO_2 ~ 75 %) operating at a pH of 8.6, IC of ~ 700 mg L^{-1} and a L/G ratio of 2 during the upgrading of a raw biogas with a composition of (% v/v) ~ 60/40 CH_4/CO_2. Mendez et al. [26] reported a biomethane CO_2 concentration of 6 % v/v (RE-CO_2 ~ 87 %) at a pH = 8.3, IC ~ 500 mg L^{-1} and L/G ratio = 2 in a similar absorption column fed with a raw biogas composition of (% v/v) ~ 65/35 CH_4/CO_2. Likewise, Vargas-Estrada et al. [24] reported CO_2 contents in the biomethane of 6.3 % v/v (RE-CO_2 ~ 82 %) at a pH of 8.5, IC of ~ 600 mg L^{-1} and L/G ratio of 2 with a raw biogas composition of (% v/v) ~ 70/29.5 CH_4/CO_2 in a similar experimental set-up. Our study demonstrated that process operation with low alkalinities and L/G ratios can support RE-CO_2 > 98 % and biomethane CO_2 compositions < 1 % due to the increase in pH of the cultivation medium in the HRAP attributed likely to the increase in microalgae photosynthetic activity driven by the addition of

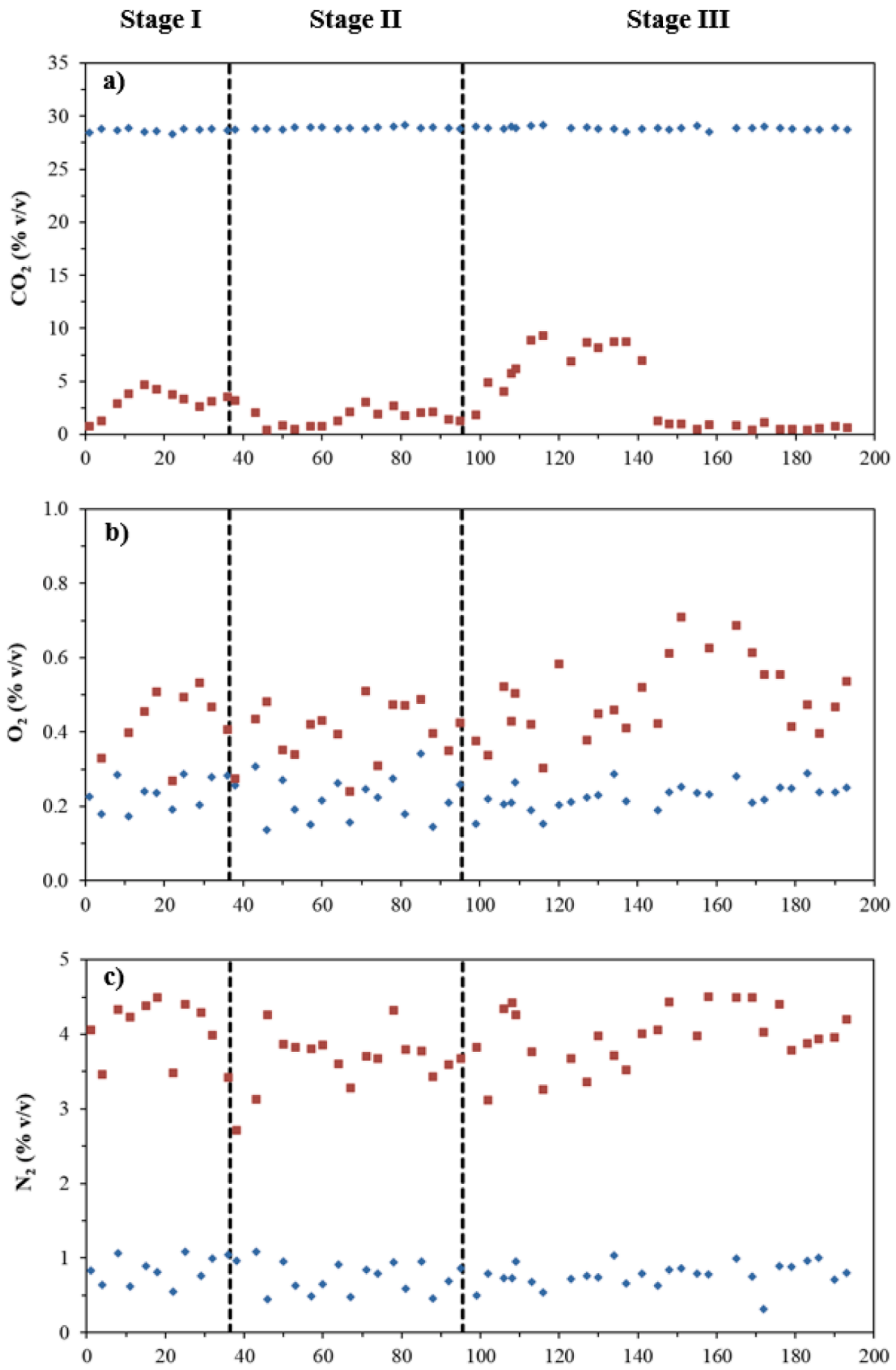

Fig. 5. Time course of a) CO_2, b) O_2, c) N_2 and d) CH_4 concentrations at the inlet (blue diamonds) and outlet (red squares) of the biogas absorption column. NPs concentration: Stage I → 70 mg L^{-1}, Stage II → 140 mg L^{-1} and Stage III → 280 mg L^{-1}.

nanoparticles.

H_2S was completely removed from biogas due to its high aqueous solubility (Henry's law constant of H_2S is approximately three times higher than that of CO_2), regardless of the nanoparticle concentration tested [19]. Overall, the average concentrations of O_2 (Fig. 5b) and N_2 (Fig. 5c) in the biomethane throughout the three operational stages were 0.5 ± 0.1 % and 3.9 ± 0.4 %, respectively. The concentration of N_2 in the biomethane is directly governed by the L/G ratio since N_2 is an inert gas that just strips out in the AC and gets absorbed from the atmosphere in the HRAP. Hence, the higher the L/G ratio (higher recirculating liquid flowrates per biogas flowrate), the higher the N_2 stripping and N_2 concentration in the biomethane. The average N_2 content in the biomethane recorded herein was in accordance with [39] using the same L/G ratio. In addition, the low O_2 content in the biomethane was supported by the reduced O_2 stripping caused by the active oxidation of H_2S to SO_4^{2-} by aerobic sulphur-oxidizing bacteria [19] and the oxygenic respiration of the algal-bacterial biomass in the absence of light in the column [26]. The low O_2 concentration achieved herein compared to previous studies, which have used similar operating conditions such as a L/G ratio of 2 under DO > 8 mg O_2 L^{-1} [13,14,25], was probably because of the high concentrations of microalgal biomass prevailing in the HRAP (1.4–3.1 g L^{-1}). This entailed a very active consumption of O_2

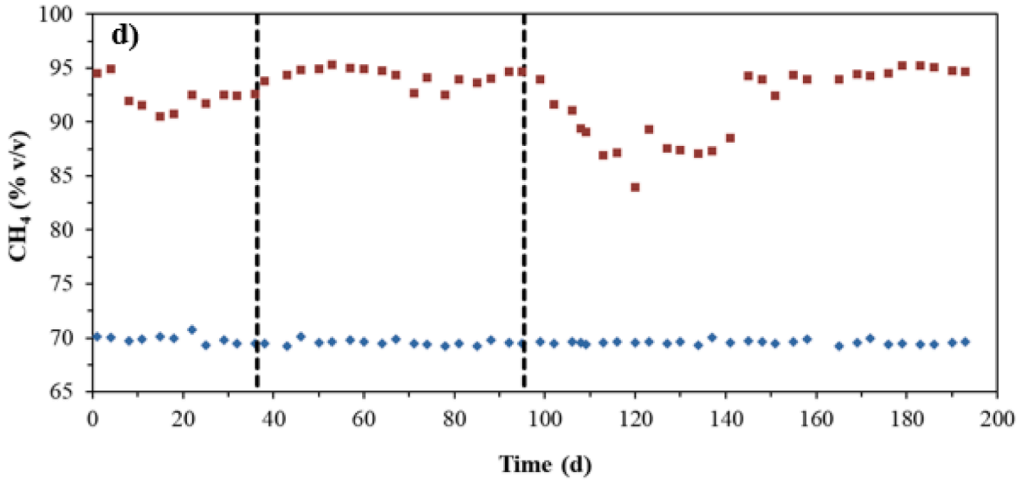

Fig. 5. (*continued*).

in the absorption column due to microbial endogenous respiration, which minimized the O_2 stripping from the culture broth to the upgraded biogas. Another reason could have been the higher biogas flowrate set in our experiment (42 ml min^{-1}) compared to the previous studies mentioned (20–30 ml min^{-1}), which implied a shorter gas–liquid contact times in the absorption column and, consequently, a lower oxygen desorption.

Finally, the CH_4 contents in the biomethane under steady state accounted for 92.4 ± 1.4 %, 94.3 ± 0.8 % and 94.4 ± 0.7 % (days 145–194) during stages I, II and III, respectively (Fig. 5d). The biomethane obtained here complied with most international regulations ($CH_4 \geq 90$ %, $CO_2 \leq 2$–4 %, $O_2 \leq 1$ %, and negligible amounts of H_2S) to be used as a substitute of natural gas for injection into natural gas grids or use in transportation [12,40]. In this sense, Marín et al. [19] achieved a biomethane with CH_4 concentration > 96 % (CO_2 content < 1 %, RE-CO_2 > 97 %) operating at pH ~ 9.5, alkalinity ~ 1250 mg IC L^{-1} and L/G ratio of 1. On the other hand, Mendez et al. [26], operating at pH ~ 9.2, alkalinity ~ 1100 mg IC L^{-1} and L/G ratio of 2, achieved a CH_4 content > 91 % (CO_2 concentration < 2.5 %, RE-CO_2 > 95 %) in the upgraded biogas. Compared to previously published control conditions [24], the strategy of NPs supplementation entailed a substantial decrease in the biomethane CO_2 composition from 6.3 to 0.8 % (RE-CO_2 increased from 86.2 to 98.1 %) and an important increase in the biomethane CH_4 composition from 83.9 to 94.4 %.

3.3. *Influence of NPs concentrations on the CO_2 gas–liquid mass transfer in the biogas absorption column*

It is well proven that nanomaterials such as nanoparticles can be properly used for gas purification and capture, as well as to enhance gas–liquid mass transfer due to their specific physicochemical properties, large active surface area per unit volume or mass and high adsorption capacity [41]. For instance, silica nanoparticles significantly increased the volumetric mass transfer coefficient (k_La) in the CO_2/water system [42]. Kim et al. [43] considerably enhanced bioethanol production in syngas fermentation by remarkably improving gas–liquid mass transfer of syngas using nanoparticles. These facts promoted the study on the influence of the NPs tested on the CO_2 gas–liquid mass transfer in the AC.

According to the results obtained in this study (Table 2), no significant differences in the pH of the liquid at the outlet of the AC were observed among the control scenario and the scenarios with NPs concentrations of 70, 150 and 300 mg L^{-1}. On the contrary, significant differences in the CO_2 gas concentration at the outlet of the AC were observed among the control scenario and the scenarios with NPs concentrations. However, these differences were probably due to experimental errors since the largest difference from control conditions was 3.5 % (at a NPs concentration of 70 mg L^{-1}) and therefore the influence of NPs on CO_2 absorption in the AC was negligible. This can be explained by the zero affinity of the nanoparticles studied for CO_2 and therefore no possibility of CO_2 adherence on the nanoparticle surface to improve mass transfer. Another hypothesis for the absence of enhancement in the CO_2 gas–liquid mass transfer in the absorption column when adding NPs (contrary to the results obtained by Vargas-Estrada et al. [24], in which the volumetric mass transfer coefficient was improved by 44 %) is that equilibrium conditions had already been reached in the control scenario, so there was no room for improvement, unless some equilibrium parameter would have been modified. H_2S was completely absorbed in the liquid because of its high aqueous solubility. Interestingly, O_2 and N_2 gas concentrations at the outlet of the AC significantly decreased when NPs were added (decrease by 20–30 % for O_2 and 10–20 % for N_2 compared to control test) but did not follow a clear trend with increasing NPs concentration. The decrease in the O_2 and N_2 content in the biogas after absorption column mediated by the addition of the nanoparticles was in accordance with [24]. These findings confirmed that the improvement in the RE-CO_2 in the AC by the addition of NPs studied is not based on an enhancement in the CO_2 gas–liquid mass transfer but rather on an upgrading in the equilibrium conditions due to the increase in the pH of the culture broth caused by the improvement in photosynthesis.

Table 2
Influence of NPs concentrations on the CO_2 gas–liquid mass transfer in the abiotic biogas absorption column.

	NPs concentration (mg L^{-1})			
	0	70	150	300
pH	7.59 ± 0.05	7.57 ± 0.03**	7.60 ± 0.01**	7.57 ± 0.03**
CO_2 (% v/v)	8.5 ± 0.1	8.2 ± 0.1*	8.7 ± 0.1*	8.6 ± 0.1*
O_2 (% v/v)	2.2 ± 0.1	1.7 ± 0.1*	1.5 ± 0.1*	1.7 ± 0.1*
N_2 (% v/v)	4.7 ± 0.1	4.1 ± 0.3*	3.8 ± 0.2*	4.2 ± 0.2*
CH_4 (% v/v)	84.6 ± 0.1	86.0 ± 0.3*	86.0 ± 0.2*	85.5 ± 0.3*

Mean values ± standard deviation were obtained from 5 measurements under steady state.
* $p < 0.05$ compared to control test.
** $p > 0.05$ compared to control test.

4. Conclusions

To the best of the author' knowledge, this is the first experimental study evaluating the effect of carbon-coated zero-valent iron-based nanoparticle concentrations (70, 140 and 280 mg L^{-1}) on continuous photosynthetic biogas purification. The nanoparticle supplementation strategy allowed the quality of the biomethane produced to comply with most international regulations, achieving CO_2 composition < 1 % (RE-CO_2 > 98 %) and CH_4 composition > 94 % in the upgraded biogas at low alkalinities and L/G ratios (~500 mg IC L^{-1} and 2, respectively). This was probably due to the significant improvement of photosynthetic activity in the HRAP promoted by the addition of NPs, which managed to achieve a biomass productivity > 100 % compared to the scenario without nanoparticles. During stage III (NPs concentration of 280 mg L^{-1}), a shift in the microalgal population structure was observed probably derived from ionic strength (or alkalinity) accumulation in the cultivation broth triggered by zero effluent strategy. Finally, it was demonstrated that nanoparticle concentrations of 70, 150 and 300 mg L^{-1} had no influence on the CO_2 gas–liquid mass transfer in the biogas absorption column.

CRediT authorship contribution statement

Edwin G. Hoyos: Writing – original draft, Visualization, Validation, Methodology, Investigation, Conceptualization. **Gloria Amo-Duodu:** Methodology, Investigation. **U. Gulsum Kiral:** Investigation, Methodology. **Laura Vargas-Estrada:** Methodology, Conceptualization. **Raquel Lebrero:** Writing – review & editing, Project administration. **Raúl Muñoz:** Writing – review & editing, Validation, Supervision, Project administration, Methodology, Funding acquisition, Conceptualization.

Declaration of Competing Interest

The authors declare that they have no known competing financial interests or personal relationships that could have appeared to influence the work reported in this paper.

Data availability

The data that has been used is confidential.

Acknowledgements

This work was supported by the Regional Government of Castilla y León and the EU-FEDER programme (CLU 2017-09, CL-EI-2021-07 and UIC 315). The authors acknowledge Enrique Marcos, Beatriz Muñoz, Mónica Gay, Araceli Crespo and Saúl Blanco for their technical support and CALPECH for providing the nanoparticles.

Appendix A. Supplementary material

Supplementary data to this article can be found online at https://doi.org/10.1016/j.fuel.2023.129610.

References

[1] Sharma P, Gujjala LKS, Varjani S, Kumar S. Emerging microalgae-based technologies in biorefinery and risk assessment issues: Bioeconomy for sustainable development. Sci Total Environ 2022;813:152417. https://doi.org/10.1016/j.scitotenv.2021.152417.
[2] Vigani M. The bioeconomy of microalgae-based processes and products. In: Handbook of Microalgae-Based Processes and Products: Fundamentals and Advances in Energy, Food, Feed, Fertilizer, and Bioactive Compounds. Elsevier Inc; 2020. p. 799–821. https://doi.org/10.1016/B978-0-12-818536-0.00029-4.
[3] Reis A, Aci FG, Wijffels H, Barbosa M, Verdelho V, Llamas B. The role of microalgae in the bioeconomy. N Biotechnol 2021;61:99–107. https://doi.org/10.1016/j.nbt.2020.11.011.
[4] Acién FG, Molina E, Reis A, Torzillo G, Zittelli GC, Sepúlveda C, et al. Photobioreactors for the production of microalgae. In: Microalgae-Based Biofuels and Bioproducts: From Feedstock Cultivation to End-Products. Elsevier; 2017. p. 1–44. https://doi.org/10.1016/B978-0-08-101023-5.00001-7.
[5] Chisti Y. Raceways-based production of algal crude oil. Green 2013;3(3–4):195–216. https://doi.org/10.1515/green-2013-0018.
[6] Norsker NH, Barbosa MJ, Vermuë MH, Wijffels RH. Microalgal production - A close look at the economics. Biotechnol Adv 2011;29(1):24–7. https://doi.org/10.1016/j.biotechadv.2010.08.005.
[7] Ortiz A, Díez-Montero R, García J, Khalil N, Uggetti E. Advanced biokinetic and hydrodynamic modelling to support and optimize the design of full-scale high rate algal ponds. Comput Struct Biotechnol J 2022;20:386–98. https://doi.org/10.1016/j.csbj.2021.12.034.
[8] Hernández-Pérez A, Labbé JI. Microalgae, culture and benefits. Rev Biol Mar Oceanogr 2014;49(2):157–73. https://doi.org/10.4067/S0718-19572014000200001.
[9] Torres-Franco A, Passos F, Figueredo C, Mota C, Muñoz R. Current advances in microalgae-based treatment of high-strength wastewaters: challenges and opportunities to enhance wastewater treatment performance. Rev Environ Sci Biotechnol 2021;20(1):209–35. https://doi.org/10.1007/s11157-020-09556-8.
[10] Alcántara C, García-Encina PA, Muñoz R. Evaluation of the simultaneous biogas upgrading and treatment of centrates in a high-rate algal pond through C, N and P mass balances. Water Sci Technol 2015;72(1):150–7. https://doi.org/10.2166/wst.2015.198.
[11] Posadas E, et al. Feasibility study of biogas upgrading coupled with nutrient removal from anaerobic effluents using microalgae-based processes. J Appl Phycol 2016;28(4):2147–57. https://doi.org/10.1007/s10811-015-0758-3.
[12] Cantera S, Fischer PQ, Sánchez-Andrea I, Marín D, Sousa DZ, Muñoz R. Impact of the algal-bacterial community structure, physio-types and biological and environmental interactions on the performance of a high rate algal pond treating biogas and wastewater. Fuel 2021;302:121148. https://doi.org/10.1016/j.fuel.2021.121148.
[13] Bahr M, Díaz I, Dominguez A, González Sánchez A, Muñoz R. Microalgal-biotechnology as a platform for an integral biogas upgrading and nutrient removal from anaerobic effluents. Environ Sci Technol 2014;48(1):573–81. https://doi.org/10.1021/es403596m.
[14] Toledo-Cervantes A, Serejo ML, Blanco S, Pérez R, Lebrero R, Muñoz R. Photosynthetic biogas upgrading to bio-methane: Boosting nutrient recovery via biomass productivity control. Algal Res 2016;17:46–52. https://doi.org/10.1016/j.algal.2016.04.017.
[15] Posadas E, Marín D, Blanco S, Lebrero R, Muñoz R. Simultaneous biogas upgrading and centrate treatment in an outdoors pilot scale high rate algal pond. Bioresour Technol 2017;232:133–41. https://doi.org/10.1016/j.biortech.2017.01.071.
[16] Rodero MDR, Posadas E, Toledo-Cervantes A, Lebrero R, Muñoz R. Influence of alkalinity and temperature on photosynthetic biogas upgrading efficiency in high rate algal ponds. Algal Res 2018;33:284–90. https://doi.org/10.1016/j.algal.2018.06.001.
[17] Rodero M del R, Severi CA, Rocher-Rivas R, Quijano G, Muñoz R. Long-term influence of high alkalinity on the performance of photosynthetic biogas upgrading. Fuel 2020;281:118804. https://doi.org/10.1016/j.fuel.2020.118804.
[18] Wang F, Liu T, Guan W, Xu L, Huo S, Ma A, et al. Development of a strategy for enhancing the biomass growth and lipid accumulation of chlorella sp. UJ-3 using magnetic Fe3O4 nanoparticles. Nanomaterials 2021;11(11):2802. https://doi.org/10.3390/nano11112802.
[19] Marín D, Carmona-Martínez AA, Blanco S, Lebrero R, Muñoz R. Innovative operational strategies in photosynthetic biogas upgrading in an outdoors pilot scale algal-bacterial photobioreactor. Chemosphere 2021;264:128470. https://doi.org/10.1016/j.chemosphere.2020.128470.
[20] Rawat J, Gupta PK, Pandit S, Prasad R, Pande V. Current perspectives on integrated approaches to enhance lipid accumulation in microalgae. 3 Biotech 2021;11(6):303. https://doi.org/10.1007/s13205-021-02851-3.
[21] Vargas-Estrada L, Torres-Arellano S, Longoria A, Arias DM, Okoye PU, Sebastian PJ. Role of nanoparticles on microalgal cultivation: A review. Fuel 2020;280:118598. https://doi.org/10.1016/j.fuel.2020.118598.
[22] Vargas-Estrada L, Hoyos EG, Sebastian PJ, Muñoz R. Elucidating the role of nanoparticles on photosynthetic biogas upgrading: Influence of biogas type, nanoparticle concentration and light source. Algal Res 2022;68:102899. https://doi.org/10.1016/j.algal.2022.102899.
[23] Vargas-Estrada L, Hoyos EG, Sebastian PJ, Muñoz R. Influence of mesoporous iron based nanoparticles on Chlorella sorokiniana metabolism during photosynthetic biogas upgrading. Fuel 2023;333:126362. https://doi.org/10.1016/j.fuel.2022.126362.
[24] Vargas-Estrada L, Hoyos EG, Méndez L, Sebastian PJ, Muñoz R. Boosting photosynthetic biogas upgrading via carbon-coated zero-valent iron nanoparticle addition: A pilot proof of concept study. Sustain Chem Pharm 2023;31:100952. https://doi.org/10.1016/j.scp.2022.100952.
[25] Serejo ML, Posadas E, Boncz MA, Blanco S, García-Encina P, Muñoz R. Influence of biogas flow rate on biomass composition during the optimization of biogas upgrading in microalgal-bacterial processes. Environ Sci Technol 2015;49(5):3228–36. https://doi.org/10.1021/es5056116.
[26] Méndez L, García D, Perez E, Blanco S, Muñoz R. Photosynthetic upgrading of biogas from anaerobic digestion of mixed sludge in an outdoors algal-bacterial photobioreactor at pilot scale. J Water Process Eng 2022;48:102891. https://doi.org/10.1016/j.jwpe.2022.102891.

[27] Alcántara C, García-Encina PA, Muñoz R. Evaluation of mass and energy balances in the integrated microalgae growth-anaerobic digestion process. Chem Eng J 2013;221:238–46. https://doi.org/10.1016/j.cej.2013.01.100.
[28] Eaton AD, Clesceri LS, Greenberg AE. Standard methods for the examination of water and wastewater. 21st ed. Washington, DC: American Public Health Association/American Water Works Association/Water Environment Federation; 2005.
[29] Posadas E, Serejo ML, Blanco S, Pérez R, García-Encina PA, Muñoz R. Minimization of biomethane oxygen concentration during biogas upgrading in algal-bacterial photobioreactors. Algal Res 2015;12:221–9. https://doi.org/10.1016/j.algal.2015.09.002.
[30] Guieysse B, Béchet Q, Shilton A. Variability and uncertainty in water demand and water footprint assessments of fresh algae cultivation based on case studies from five climatic regions. Bioresour Technol 2013;128:317–23. https://doi.org/10.1016/j.biortech.2012.10.096.
[31] Posadas E, Muñoz A, García-González MC, Muñoz R, García-Encina PA. A case study of a pilot high rate algal pond for the treatment of fish farm and domestic wastewaters. J Chem Technol Biotechnol 2015;90(6):1094–101. https://doi.org/10.1002/jctb.4417.
[32] Asano T, Burton FL, Leverenz HL, Tsuchihashi R, Tchobanoglous G, Metcalf & Eddy Inc.. Water Reuse: Issues, Technologies, and Applications. 1st ed. New York: McGraw-Hill; 2007.
[33] Vaneeckhaute C, Lebuf V, Michels E, Belia E, Vanrolleghem PA, Tack FMG, et al. Nutrient Recovery from Digestate: Systematic Technology Review and Product Classification. Waste Biomass Valoriz 2017;8(1):21–40. https://doi.org/10.1007/s12649-016-9642-x.
[34] Chierici M, Vernet M, Fransson A, Børsheim KY. Net Community Production and Carbon Exchange From Winter to Summer in the Atlantic Water Inflow to the Arctic Ocean. Front Mar Sci 2019;6(September):1–24. https://doi.org/10.3389/fmars.2019.00528.
[35] Zeebe RE, Wolf-Gladrow D. CO2 in Seawater: Equilibrium, Kinetics, Isotopes. Elsevier Science; 2001.
[36] Cromar NJ, Fallowfield HJ, Martin NJ. Influence of environmental parameters on biomass production and nutrient removal in a high rate algal pond operated by continuous culture. Water Sci Technol 1996;34(11):133–40. https://doi.org/10.1016/S0273-1223(96)00830-X.
[37] Metcalf & Eddy, Inc.. Wastewater Engineering: Treatment and Reuse. 4th ed. New York: McGraw-Hill; 2003.
[38] Posadas E, Morales MDM, Gomez C, Acién FG, Muñoz R. Influence of pH and CO2 source on the performance of microalgae-based secondary domestic wastewater treatment in outdoors pilot raceways. Chem Eng J 2015;265:239–48. https://doi.org/10.1016/j.cej.2014.12.059.
[39] Marín D, Méndez L, Suero I, Díaz I, Blanco S, Fdz-Polanco M, et al. Anaerobic digestion of food waste coupled with biogas upgrading in an outdoors algal-bacterial photobioreactor at pilot scale. Fuel 2022;324:124554. https://doi.org/10.1016/j.fuel.2022.124554.
[40] Marín D, Ortíz A, Díez-Montero R, Uggetti E, García J, Lebrero R, et al. Influence of liquid-to-biogas ratio and alkalinity on the biogas upgrading performance in a demo scale algal-bacterial photobioreactor. Bioresour Technol 2019;280:112–7. https://doi.org/10.1016/j.biortech.2019.02.029.
[41] Alonso A, Moral-Vico J, Abo Markeb A, Busquets-Fité M, Komilis D, Puntes V, et al. Critical review of existing nanomaterial adsorbents to capture carbon dioxide and methane. Sci Total Environ 2017;595:51–62. https://doi.org/10.1016/j.scitotenv.2017.03.229.
[42] Jeon HS, Park SE, Ahn B, Kim YK. Enhancement of biodiesel production in Chlorella vulgaris cultivation using silica nanoparticles. Biotechnol Bioprocess Eng 2017;22(2):136–41. https://doi.org/10.1007/s12257-016-0657-8.
[43] Kim YK, Park SE, Lee H, Yun JY. Enhancement of bioethanol production in syngas fermentation with Clostridium ljungdahlii using nanoparticles. Bioresour Technol 2014;159:446–50. https://doi.org/10.1016/j.biortech.2014.03.046.